European Journal of Medicinal Chemistry 208 (2020) 112752

Contents lists available at ScienceDirect

European Journal of Medicinal Chemistry

journal homepage: http://www.elsevier.com/locate/ejmech

Novel 2-indolinone thiazole hybrids as sunitinib analogues: Design, synthesis, and potent VEGFR-2 inhibition with potential anti-renal cancer activity

Huda K. Mahmoud [a], Thoraya A. Farghaly [a, b, *], Hanan G. Abdulwahab [c], Nadia T. Al-Qurashi [d], Mohamed R. Shaaban [a, b]

[a] Department of Chemistry, Faculty of Science, Cairo University, Giza, 12613, Egypt
[b] Department of Chemistry, Faculty of Applied Science, Umm Al-Qura University, Makkah Almukkarramah, Saudi Arabia
[c] Pharmaceutical Chemistry Department, Faculty of Pharmacy (Girls), Al-Azhar University, Cairo, Egypt
[d] Department of Basic Science, University College in Adam, Umm Al-Qura University, Makkah Almukkarramah, Saudi Arabia

ARTICLE INFO

Article history:
Received 4 June 2020
Received in revised form
5 August 2020
Accepted 7 August 2020
Available online 21 August 2020

Keywords:
Indolinone
Thiazoles
Sunitinib
Anti-renal cancer activity
Docking study

ABSTRACT

Novel 2-indolinone thiazole hybrids were designed and synthesized as VEGFR-2 inhibitors based on sunitinib, an FDA-approved anticancer drug. The proposed structures of the prepared 2-indolinone thiazole hybrids were confirmed based on their spectral data and CHN analyses. The target compounds were screened *in vitro* for their anti-VEGFR-2 activity. All tested compounds exhibited a potent submicromolar inhibition of VEGFR-2 kinase with IC_{50} values ranging from 0.067 to 0.422 μM, relative to sunitinib reference drug (IC_{50} = 0.075 ± 0.002 μM). Compounds **5, 15a, 15b, 17, 19c** displayed excellent VEGFR-2 inhibitory activity, comparable or nearly equipotent to sunitinib. Compound **13b** stood out as the most potent against VEGFR-2 showing IC_{50} value of 0.067 ± 0.002 μM, lower than that of sunitinib. In addition, the most potent derivatives were assessed for their anticancer activity against two renal cancer cell lines. Compound **13b** (IC_{50} = 3.9 ± 0.13 μM) was more potent than sunitinib (IC_{50} = 4.93 ± 0.16 μM) against CAKI-1 cell line. Moreover, thiazole **15b** displayed excellent anticancer activity against CAKI-1 cell line (IC_{50} = 3.31 ± 0.11 μM), superior to that of sunitinib (IC_{50} = 4.93 ± 0.16 μM). Thiazole **15b** was also equipotent to sunitinib (IC_{50} = 1.23 ± 0.04 μM) against A498 cell line. Besides, compound **15b** revealed a safety profile much better than that of sunitinib against normal human renal cells. Furthermore, a docking study revealed a proper fitting of the most active compounds into the ATP binding site of VEGFR-2, rationalizing their potent anti-VEGFR-2 activity.

1. Introduction

Cancer is a worldwide health problem that leads to death in both developing and developed countries [1]. Even though the exploration for anticancer candidates started on the beginning of the preceding century, there is a persistent need to develop new anticancer agents to overcome the adverse effects and the resistance development associated with most marketed anticancer drugs [2]. Thus, extensive efforts have been devoted to the development of new potent chemotherapeutic agents with higher selectivity toward cancer cells [3].

In many proteins, phosphorylation of their tyrosine moiety have been achieved by catalysis of protein tyrosine kinases (PTKs). PTKs take a pivotal part in proliferation, differentiation, and migration signaling in the cell. It is well known that cancer development is associated with abnormal activation or over-expression of PTKs [4–6].

Vascular endothelial growth factor receptor-2 (VEGFR-2), a transmembrane tyrosine kinase receptor, has been recognized as the most critical factor in promoting angiogenesis [7–9]. Angiogenesis is a complex process that involves the creation of new blood vessels from the pre-existing vasculature in physiological and pathophysiological conditions. Also, angiogenesis is considered as one of the hallmarks of tumor growth, invasion and metastasis [10–12]. Playing a central role in cancer pathophysiology, VEGFR-2 is well-established as the supreme significant target in anti-

* Corresponding author. Department of Chemistry, Faculty of Science, Cairo University, Giza, 12613, Egypt.
E-mail addresses: thoraya-f@hotmail.com, tamohamed@uqu.edu.sa (T.A. Farghaly).

https://doi.org/10.1016/j.ejmech.2020.112752
0223-5234/

angiogenesis therapy against cancer. In this context, several small molecule VEGFR-2 inhibitors have been clinically approved or tested for cancer treatment (Fig. 1) [13–15].

Indolin-2-one scaffold attracted considerable attention towards anticancer research, particularly the discovery of protein kinase inhibitors [16,17]. Moreover, 2-indolinone derivatives were among the initial structures recognized as kinase inhibitors and have been thoroughly investigated for the inhibition of VEGFR (Fig. 1) [18]. Sunitinib (Fig. 1) is the first kinase inhibitor of the indolinone category that reached the market. It is indicated for the treatment of renal cell carcinoma and imatinib-resistant gastrointestinal stromal tumor. Sunitinib binds to the kinase domain of VEGFR-2 and inhibits its activity [19].

On the other hand, thiazole is a fascinating heterocyclic core in medicinal chemistry for the design and discovery of bioactive compounds, particularly, anticancer agents [20–22]. Many thiazoles have been specially designed to target specific pathways that are involved in cancer pathogenesis [20–22]. For example, the FDA-approved thiazole-containing drugs, dabrafenib and dasatinib, are selective tyrosine kinase inhibitors with very potent antitumor activity (Fig. 2) [23,24].

Encouraged by these findings and in continuation of our ongoing study project in designing and synthesis of novel biologically active heterocyclic compounds [25–30], novel 2-indolinone thiazole hybrids were designed and synthesized as sunitinib analogues with prospective VEGFR-2 inhibitory activity. The approach utilized for designing our target candidates is illustrated in Fig. 3.

In the present work, while conserving the indolinone core of sunitinib, a benzyl moiety was introduced to the nitrogen atom of the indolinone core to improve binding affinity towards VEGFR-2 active site *via* hydrophobic interactions. Surveying literature revealed that the improvement of the binding affinity towards VEGFR-2 active site has been attained through the increase of the hydrophobic interactions with the hydrophobic pockets of the VEGFR-2 active site e.g. vatalanib and sorafenib (Fig. 1) [31,32]. It was also reported that the introduction of hydrophobic moieties to the 2-indolinone core resulted in enhanced binding affinity and so improved kinase inhibitory activity [33]. In this work, fluorine atom in sunitinib was also replaced by its chlorine bioisostere. Additionally, simplification approach was also employed to obtain compounds **3** and **5**. Furthermore, the substituted pyrrole in sunitinib was replaced by substituted thiazole/thiazolidinone ring as represented in target compounds **10a-c, 15a,b, 17** and **19a-c**. Compounds **13a-c** were synthesized as open thiazolidinone analogues with different substituents at *para*-position of phenyl ring. Moreover, substituents of diverse size and electronic properties were introduced to position 4 and 5 of thiazole ring in compounds **10a-c, 15a,b** and **19a-c** to explore their impact on VEGFR-2 inhibitory activity. To study the effect of linker extension on anti-VEGFR-2 activity, the CH linker in sunitinib was also replaced by a hydrogen-bond acceptor and relatively longer (=N–N=) linker in compounds **10**–**19**.

All targeted products were screened for their in vitro VEGFR-2 inhibitory activity. Furthermore, the most potent derivatives were further assessed in vitro for their anticancer activity against two renal cancer cell lines. A docking study was also conducted to predict the binding mode of the promising compounds within the binding site of VEGFR-2 kinase.

2. Results and discussion

2.1. Chemistry

The versatile starting substrate 1-benzyl-5-chloroindoline-2,3-dione (**2**) was prepared by treatment of 5-chloroisatin (**1**) with benzyl chloride in DMF with stirring at room temperature using

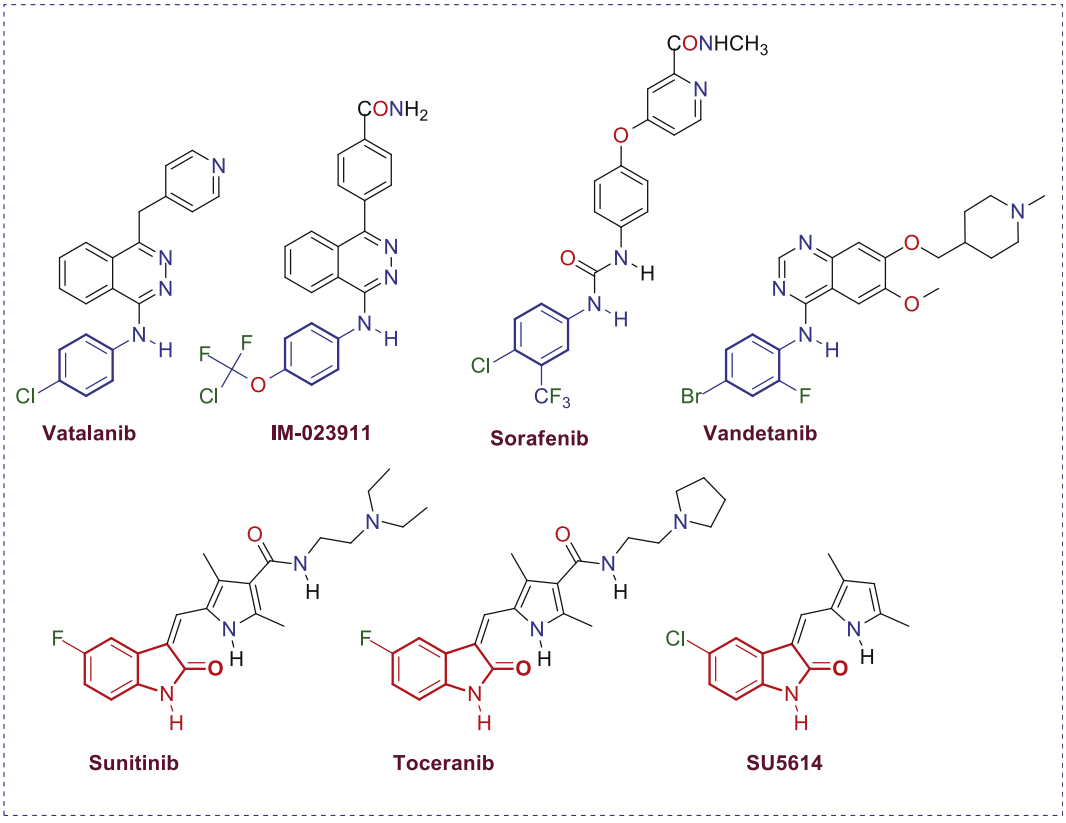

Fig. 1. Clinically approved/tested VEGFR-2 inhibitors.

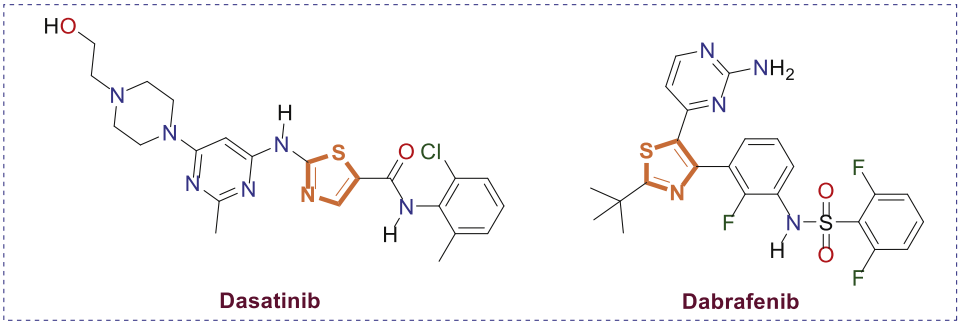

Fig. 2. Clinically approved thiazole-containing tyrosine kinase inhibitors.

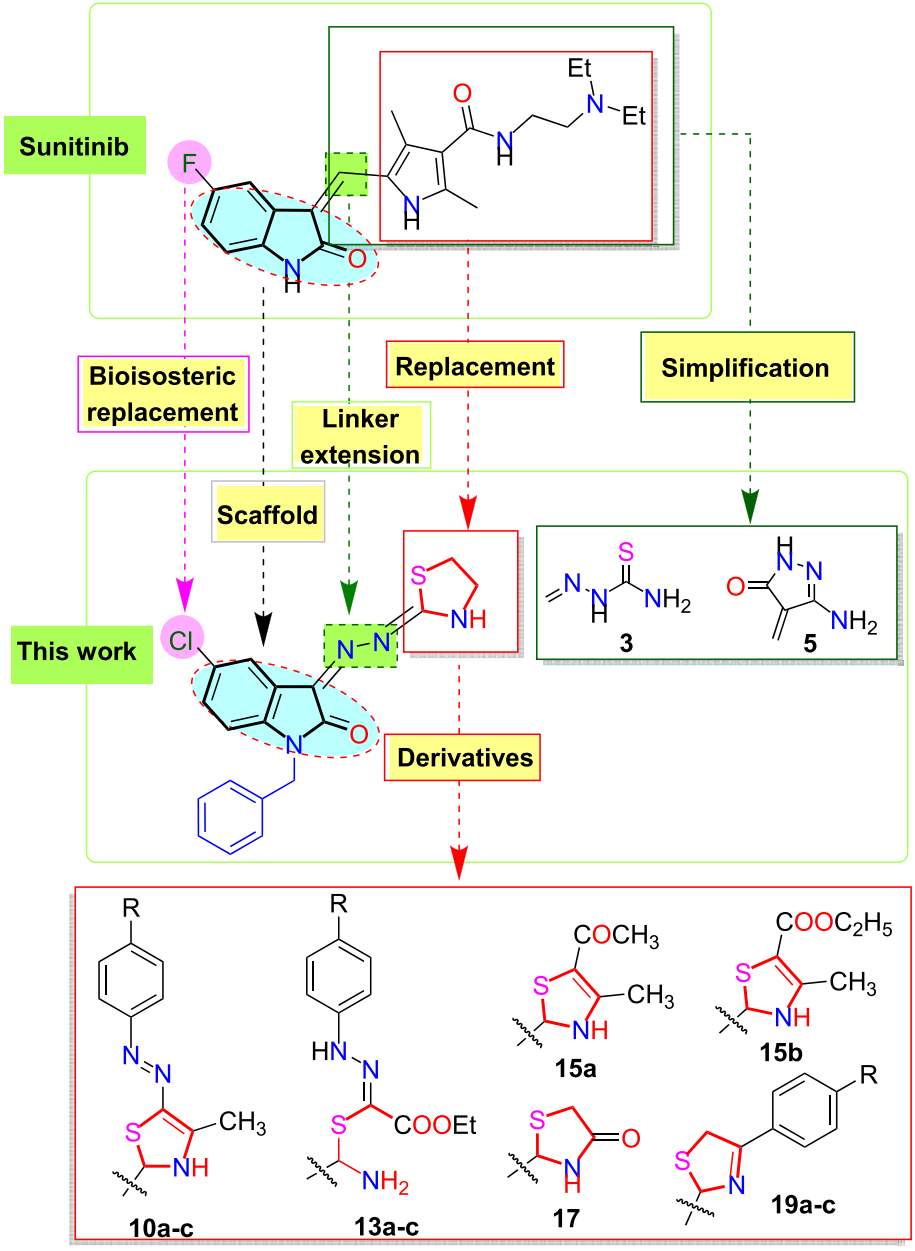

Fig. 3. Design of target compounds based on Sunitinib VEGFR-2 inhibitor.

potassium carbonate as a catalyst following to reported procedure [34] as shown in Scheme 1. The utility of the 1-benzyl-5-chloroindoline-2,3-dione (**2**) in the synthesis of multifunctional building blocks have been initiated by refluxing compound **2** and thiosemicarbazide using ethanol containing HCl for 4 h as depicted in Scheme 1 and reported in literature [34]. Condensation proceeded to afford the corresponding the thiosemicarbazone derivative **3** in 81% yield. On the other hand, a mixture of 1-benzyl-5-chloroindoline-2,3-dione **2** and cyanoacetic acid hydrazide (**4**) in ethanol/acetic acid solvent mixture was refluxed to give the amino pyrazolone derivative **5** instead of the cyanoacetohydrazide derivative **6** as depicted in Scheme 1. The formation of 1*H*-pyrazolylidene derivatives **5** was confirmed by the extracted data from ^{1}H NMR and IR as shown in Figs. 4 and 5. For detailed, the appearance of D_2O-exchangeable broad signal at δ 4.42 ppm with integration equivalent to NH_2 group protons in ^{1}H NMR confirmed structure **5** rather than the acyclic isomer **6** as illustrated in Fig. 4. Another evidence comes from its IR spectrum (Fig. 5) which free from the cyano group (C≡N) absorption at $\nu \approx 2200$ cm^{-1}. The formation of compound **5** proceeded through the nucleophilic condensation reaction with elimination of H_2O from the active methylene CH_2 group of the cyano acid hydrazide **4** and the carbonyl group of substituted isatin **2** followed by cyclization *via* the nuecleophilic addition reaction (*Mickle type* addition reaction) of the amino group to the C≡N.

The targeted 2-indolinone incorporated arylazothiazole derivatives **10a-c**, were synthesized by condensation of the 2-indolinone-based thiosemicarbazone derivative **3** with *C*-acetyl-2-oxo-*N*-arylpropanehydrazonoyl chlorides **7a-c** in dioxane and using TEA as a basic catalyst (Scheme 2). The novel 2-indolinone-thiazole hybrid derivatives **10a-c** were obtained in 79–86% yield under this applied reaction conditions. The structure of 2-indolinone-thiazole hybrid derivatives **10a-c** were confirmed by their spectral and microanalyses. All ^{1}H NMR spectra of the thiazole derivatives **10a-c** were characterized with the existence of only one NH singlet signal at $\delta = 11.2$–13.19 ppm in addition to the aromatic protons, moreover, the aliphatic region in the ^{1}H NMR of derivatives **10b** and **10c** characterized with the appearance of two singlet signals of each at $\delta = 2.62$ (CH_3), 3.82 (OCH_3), 2.37 (CH_3) and 2.65 (CH_3), respectively. The reaction of carbothioamide **3** with hydrazonoyl chlorides **7a-c**, started with nucleophilic substitution of the carbothioamide function in **3** through the sulfur atom reaction to form the intermediates **8** as shown in Scheme 2. Cyclization of intermediate **8** with elimination of water molecule (H_2O) through the non-isolable intermediate **9** gave the final products **10a-c** (Scheme 2).

Using the same reaction conditions, attempts to access the thiazolones **12a-c**, *via* one pot reaction of 2-indolinone-based thiosemicarbazone derivative **3** with *C*-ethoxycarbonyl-*N*-arylpropanehydrazonoyl chlorides **11a-c** in the presence of TEA (Scheme 3) have been investigated. Condensation proceeded to afford the corresponding amidrazone derivatives **13a-c** rather than the expected thiazolone derivatives **12a-c**. The molecular ion peak of all mass spectra of derivatives **13a-c** proved liberation of only HCl molecule from the starting compounds **3** and **11**. Furthermore, ^{1}H NMR spectra of all amidrazone derivatives **13a-c** revealed the two signals (*t* and *q*) for the CH_3CH_2 of the ester moiety near the regions δ 1.35 and 4.40 ppm as well as the singlet signal of NH_2 group at δ 3.60 ppm in addition to aliphatic and aromatic protons. Fig. 6 represents the ^{1}H NMR of derivative **13c**. Such data confirmed the structure **13(I)** rather than the isomer form **13(II)** as illustrated in Scheme 3.

Functionalized thiazole derivatives **15a,b** have been accessed by the reaction between 2-indolinone-based thiosemicarbazone derivative **3** and α-chloro-dicarbonyl compounds **14a,b** in dioxane and using triethylamine as a catalyst as depicted in Scheme 4. The structure of the reaction products **15a,b** has been elucidated by spectral data evidences as well as elemental analyses. The IR

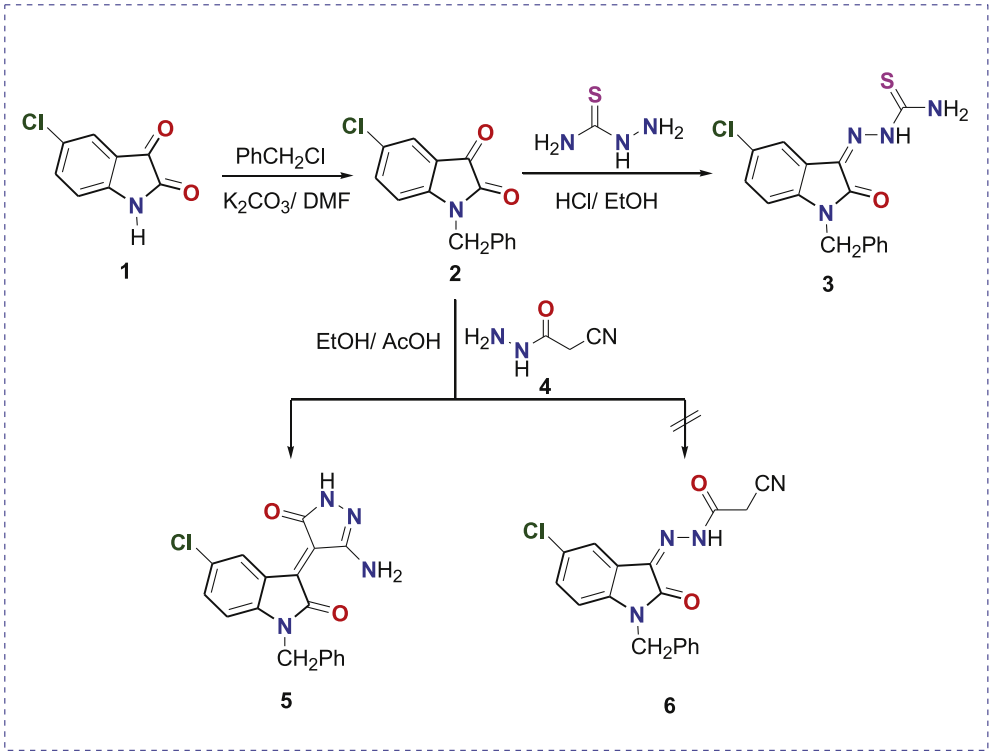

Scheme 1. Synthesis of the starting thiosemicarbazone derivative **3** and 3-(3-amino-5-oxo-1*H*-pyrazol-4(5*H*)-ylidene)-1-benzyl-5-chloroindolin-2-one (**5**).

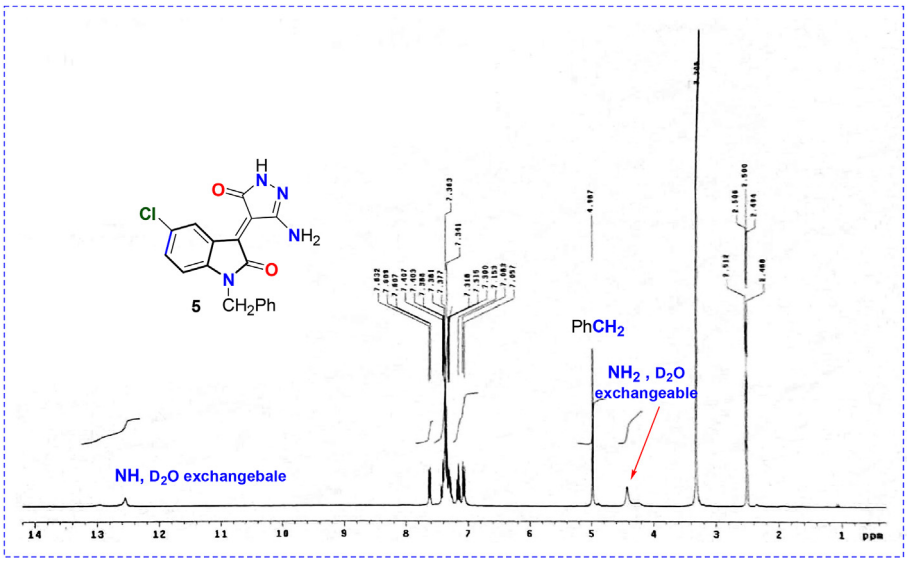

Fig. 4. The ^{1}H NMR spectrum of 3-(3-amino-5-oxo-1*H*-pyrazol-4(5*H*)-ylidene)-1-benzyl-5-chloroindolin-2-one (**5**).

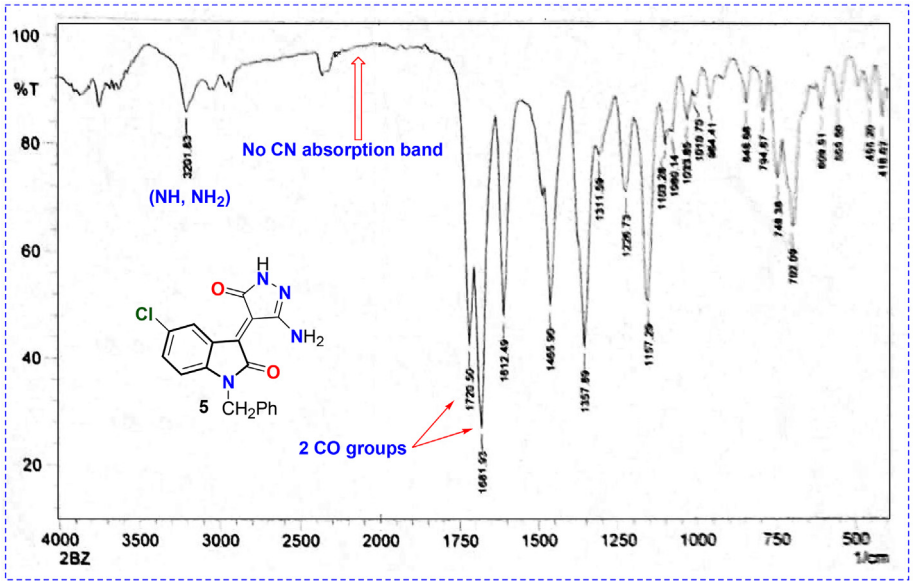

Fig. 5. The IR spectrum of 3-(3-amino-5-oxo-1*H*-pyrazol-4(5*H*)-ylidene)-1-benzyl-5-chloroindolin-2-one (**5**).

spectrum of thiazoline derivative **15**b (taken as an example) displayed a broad absorption band at 3448 cm^{-1} corresponding to the NH functions. ^{1}H NMR spectrum of compound **15b** revealed the characteristic proton signals at δ 1.03 (t), 2.49 (s), 4.24 (q), 4.99 (s), 6.92−8.30 (m), 13.16 (s) ppm assigned to the $\underline{CH_3}CH_2$, CH_3 $CH_3\underline{CH_2}$, $Ph\underline{CH_2}$, aromatic protons and NH groups, respectively.

Finally, 2-indolinone-based thiosemicarbazone derivative **3** reacts with ethyl chloroacetate (**16**) in fused sodium acetate/acetic acid mixture to give the targeted thiazolone derivative **17** as shown in Scheme 5. The structure elucidation of thiazolone derivative **17** has been achieved by spectral data and elemental analyses. In a similar manner, reaction between 2-indolinone-based thiosemicarbazone derivative **3** and phenacyl bromide derivatives **18a-c** in the presence of triethylamine afforded the corresponding thiazole derivatives **19a-c** as shown in Scheme 5. Such thiazole derivatives **19** can present in one of the tautomeric structures **19(I)** or **19(II)** (Scheme 5), the ^{1}H NMR data of these derivatives assured the form **19(I)** in the solution state. This is due to the appearance of two CH_2 groups for the thiazole-CH_2 and $PhCH_2$ at δ 4.87 and 5.04 ppm. While, the IR spectra of derivatives **19a-c** revealed the broad band at 3417-3471 cm^{-1} indicated the presence of the isomer **19(II)**. For all thiazole derivatives **19a**−**c**, the mass spectrometry results revealed the molecular ion peaks at the exact *m/z* values.

2.2. Biological activity

2.2.1. In vitro VEGFR-2 inhibition

In the present work, the title compounds were tested *in vitro* for their ability to inhibit VEGFR-2 enzyme using sunitinib as a reference drug. The screening data are presented in Table 1.

As shown in Table 1, all tested compounds effectively inhibited VEGFR-2 activity with IC_{50} values in the submicromolar level ranging from 0.067 to 0.422 μM, relative to sunitinib reference drug (IC_{50} = 0.075 ± 0.002 μM). Compounds **5, 15a,b, 17, 19c** displayed

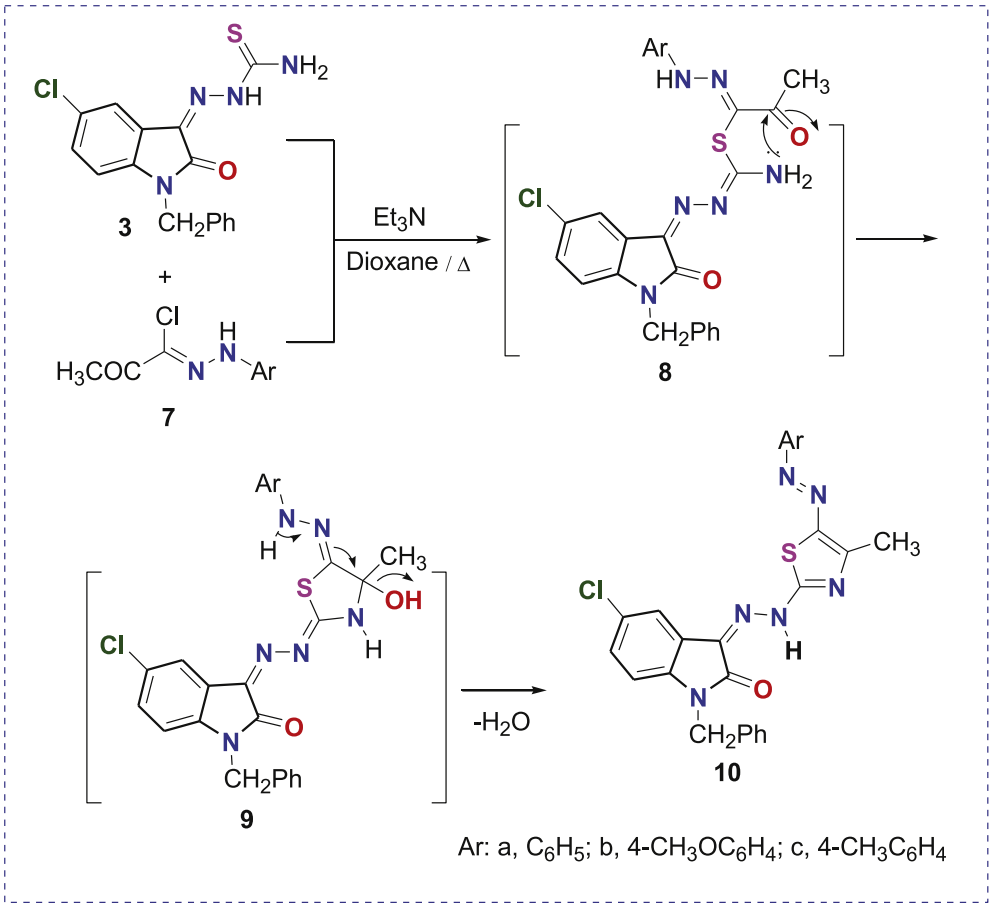

Scheme 2. Reaction of 2-(1-benzyl-5-chloro-2-oxoindolin-3-ylidene)hydrazine-1-carbothioamide (**3**) with *C*-acetyl-2-oxo-*N*-arylpropanehydrazonoyl chlorides **7a-c**.

excellent VEGFR-2 inhibitory activity (IC_{50} = 0.084 ± 0.002, 0.092 ± 0.003, 0.078 ± 0.002 and 0.088 ± 0.002 μM, respectively), comparable or nearly equipotent to sunitinib. Additionally, compounds **13a** and **13c** exhibited high VEGFR-2 inhibitory activity with IC_{50} = 0.102 ± 0.003 and 0.133 ± 0.004 μM, respectively. Furthermore, compounds **10c** and **19b** revealed half potency of sunitinib against VEGFR-2 kinase with IC_{50} = 0.153 ± 0.004 and 0.158 ± 0.004 μM, respectively. Equal VEGFR-2 inhibitory activity was also detected for compounds **3** and **10b**. Among the tested compounds in this study, compound **13b** emerged as the most potent derivative with IC_{50} = 0.067 ± 0.002 μM, lower than that of sunitinib reference drug. While, compounds **10a** and **19a** were the least potent with IC_{50} = 0.263 ± 0.007 and 0.422 ± 0.011 μM, respectively.

Examining screening results revealed that simplification approach was beneficial for VEGFR-2 inhibitory activity as indicated by the nearly equipotent activity of pyrazole derivative **5** to sunitinib. Besides, the semicarbazone open analogue **3** displayed half potency of sunitinb. It is worth mentioning that pyrazole-containing VEGFR tyrosine kinase inhibitors such as axitinib and pazopanib have been approved by FDA for the treatment of renal cell carcinomas [35].

Regarding 5-aryldiazenyl thiazole derivatives **10a-c**, 4-methyoxy (**10b**) and 4-methyl (**10c**) phenyl derivatives showed significant VEGFR-2 inhibitory activity with IC_{50} = 0.175 ± 0.005 and 0.153 ± 0.004 μM, respectively; much better than that of the unsubstituted phenyl analogue **10a**.

Comparing to thiazoles **10a-c**, arylhydrazono derivatives **13a-c**; designed as open thiazolidinone analogues, displayed better anti-VEGFR-2 activity with IC_{50} values ranging from 0.067 to 0.133 μM. Compound **13a**; bearing 4-nitrophenyl moiety, was more potent than its 4-bromophenyl analogue **13c**. Among the tested compounds, 4-tolyl hydrazono derivative **13b** stood out as the most active derivative against VEGFR-2 tyrosine kinase with IC_{50} value = 0.067 ± 0.002 μM, lower than that of sunitinib reference drug. Besides, **13b** was also two times more potent than its 4-tolyl diazenylthiazole counterpart **10c**.

Noticeably, compounds **15a** and **15b** presented potent VEGFR-2 tyrosine kinase inhibitory activity comparable to that of sunitinib with acetylthiazole **15a** being more potent than its ethyl carboxylate counterpart **15b**. Moreover, thiazolidinone analogue **17** showed better anti-VEGFR-2 activity; almost equipotent to sunitinib.

Concerning 4-arylthiazole derivatives **19a-c**, the addition of electron withdrawing chlorine atom to the *para* position of phenyl ring in compound **19b** resulted in more than two times increase in VEGFR-2 inhibitory activity compared to the unsubstituted phenyl derivative **19a**. Further increase in potency (approximately five times compared to **19a**) was obtained upon the introduction of the more electron withdrawing nitro group in compound **19c**.

Generally, it could be concluded that the introduction of a large bulky aryldiazenyl moiety to position 5 of thiazole ring is not beneficial for VEGFR-2 kinase inhibitory activity as indicated by the lower potency of compounds **10a-c** comparing to their 5-acetyl **15a** and 5-ethyl carboxylate **15b** analogues. Similarly, small methyl group at position 4 of thiazole ring in compounds **15a** and **15b** is more tolerated than relatively larger phenyl and chlorophenyl moieties in compounds **19a** and **19b**, respectively.

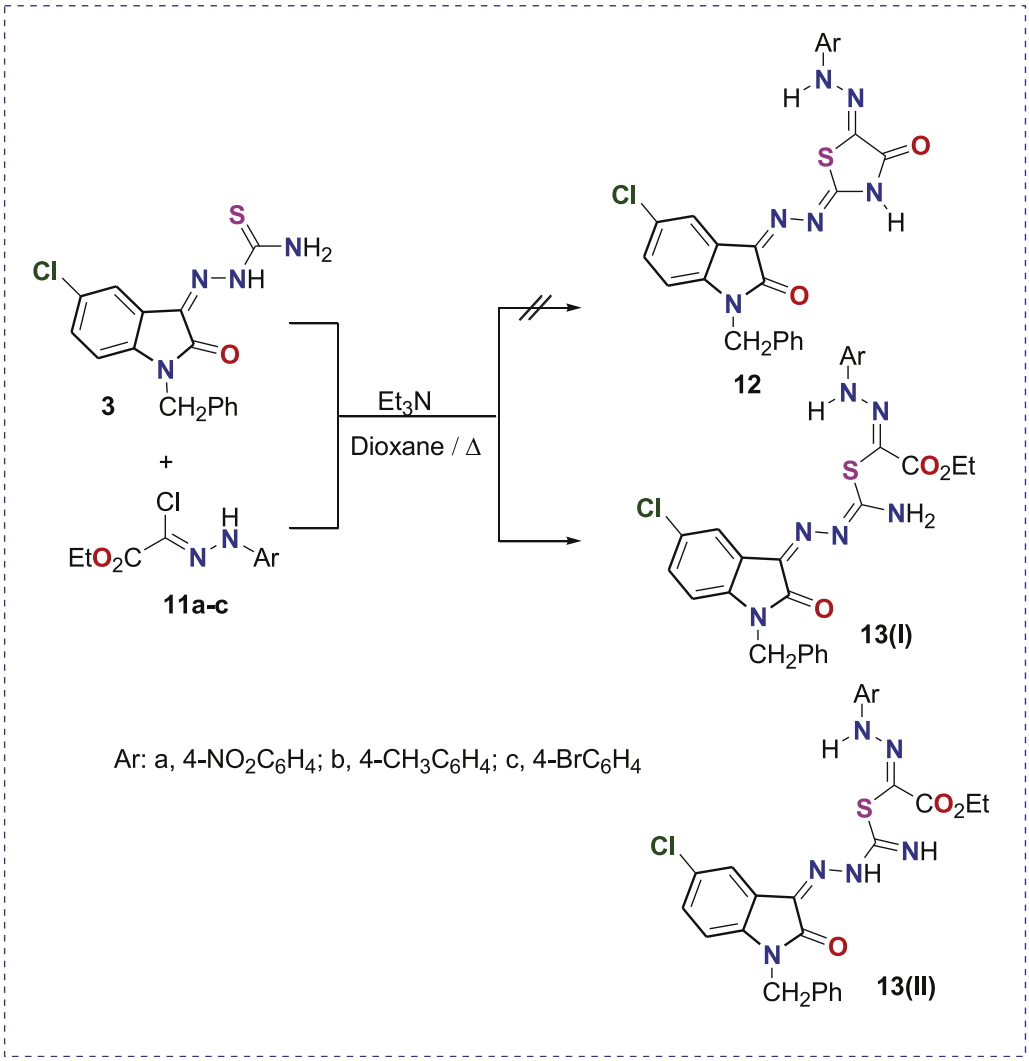

Scheme 3. The reaction of 2-(1-benzyl-5-chloro-2-oxoindolin-3-ylidene)hydrazine-1-carbothioamide (**3**) with *C*-ethoxycarbonyl-*N*-arylpropanehydrazonoyl chlorides **11a-c**.

2.2.2. In vitro anticancer activity

As mentioned above, sunitinib is clinically used for the treatment of renal cell carcinomas which are highly vascular tumors, and therefore the effectiveness of sunitinib against renal cancer is mainly attributed to the inhibition of VEGFR-2 [36]. With this in mind, the most active compounds in anti-VEGFR-2 assay; **5, 13b, 15a, 15b, 17** and **19c** were passed on to further evaluation of their *in vitro* cytotoxic activity against two human renal cancer cell lines, namely, CAKI-1 and A498 using MTT-based cytotoxicity assay [37]. Sunitinib was used as a reference drug (Table 2).

CAKI-1 and A498 cancer cell lines were obtained from American Type Culture Collection. CAKI-1 is a widespread model of renal cell carcinoma that is associated with high production of vascular endothelial growth factor. In addition, A498 is a renal cancer cell line belonging to NCI-60 panel and so is used extensively in renal cancer research [38].

From the obtained results (Table 2), it can be observed that the tested compounds displayed moderate to potent cytotoxicity against CAKI-1 and A498 cell lines with IC_{50} values ranging from two-digit micromolar to submicromolar concentrations compared to sunitinib reference drug.

Interestingly, aminopyrazolone **5** with $IC_{50} = 0.82 \pm 0.03$ μM exhibited a highly potent cytotoxic activity against CAKI-1 renal cancer cell line that was six folds more potent than sunitinib reference drug. Compound **5** also suppressed the growth of A498 renal cancer cell line at one-digit micromolar IC_{50} value of 8.53 ± 0.28 μM.

Compound **13b**, which was the most potent in anti-VEGFR-2 assay, showed cytotoxic activity against CAKI-1 cell line higher than that of sunitinib. Besides, compound **13b** efficiently inhibited the growth of A498 cell line at low micromolar IC_{50} value of 2.88 ± 0.09 μM.

In addition, thiazole **15a** effectively inhibited the growth of the two tested cell lines; however A498 cell line was two times more sensitive to thiazole **15a** than CAKI-1 cell line.

Remarkably, it was observed that the replacement of acetyl group in thiazole **15a** by ethyl carboxylate moiety in compound **15b** led to more than four times increase in cytotoxic activity. Thiazole **15b** revealed excellent anticancer activity against CAKI-1 renal cancer cell line, superior to that of sunitinib. Moreover, thiazole **15b** emerged as the most potent compound against A498 renal cancer cell line with cytotoxic activity equipotent to that of sunitinib.

On the contrary, the replacement of thiazole ring in compounds **15a** and **15b** by thiazolidinone ring in compound **17** resulted in a marked decline in growth inhibitory activity against CAKI-1 cell line. However, A498 cell line was much more sensitive to thiazolidinone **17**.

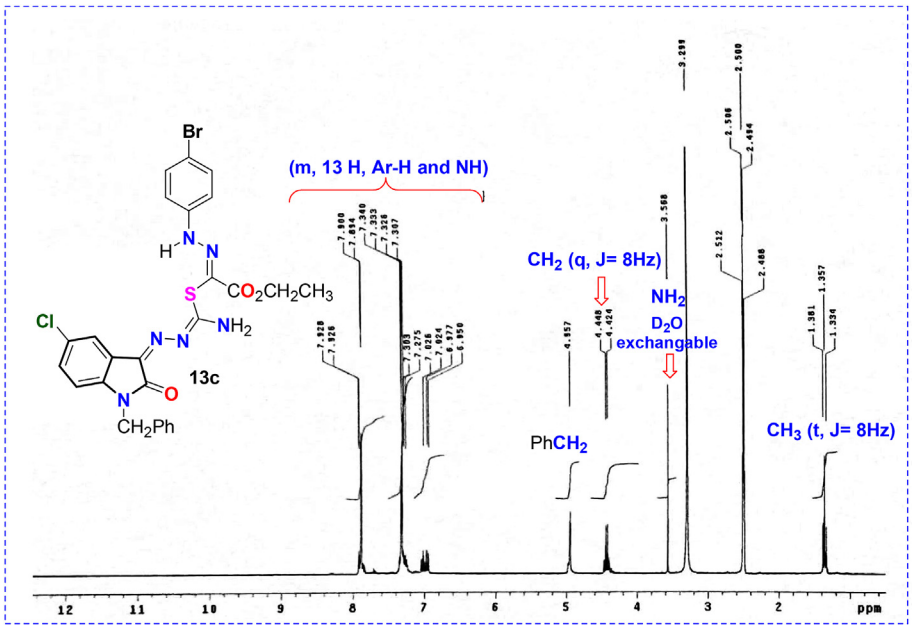

Fig. 6. The ^{1}H NMR spectrum of compound **13c**.

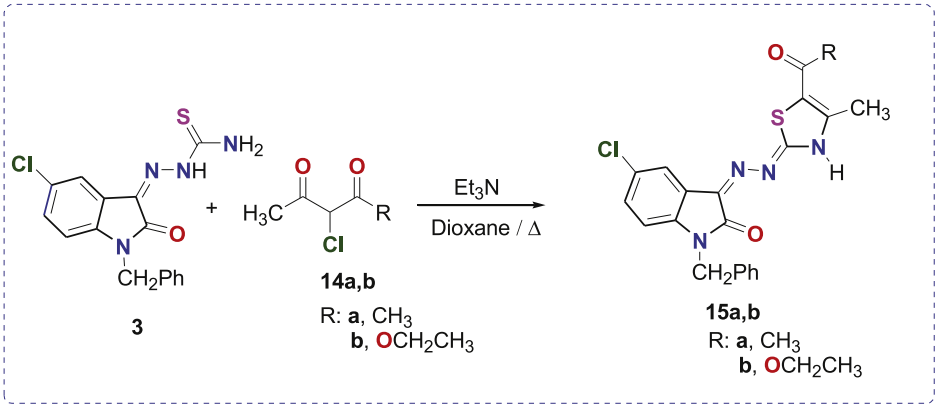

Scheme 4. Synthesis of thiazole derivatives **15a,b**.

Finally, thiazole derivative **19c**; bearing 4-nitrophenyl at position 4 of thiazole ring, demonstrated cytotoxic activity against CAKI-1 cell line comparable to that of sunitinib with IC_{50} values of 5.78 ± 0.19 and 4.93 ± 0.16 μM, respectively. However, A498 cell line was less sensitive to compound **19c**.

Notably, it could be concluded that cyclized (thiazole) analogues with relatively small substituents at position 4 and 5 of thiazole ring are beneficial for both *in vitro* VEGFR-2 inhibition and anticancer activity as indicated by the potent anti-VEGFR-2 activity and superior cytotoxicity elicited by thiazole **15b.**

2.2.3. *In vitro cytotoxicity against normal human cells*

The safety profile of the most effective analogue in this study; **15b** was also assessed by testing its *in vitro* cytotoxicity against RPTEC/TERT1 normal human cells, comparing to sutininb reference drug. RPTEC/TERT1 cells are human renal epithelial cells that are employed as a model for basic kidney functions and are also used to study nephrotoxicity [38]. It was found that compound **15b** demonstrated a safety profile much better than that of sunitinib with IC_{50} values of 49.8 ± 2.79 and 16.9 ± 0.95 μM, respectively.

2.2.4. *Docking study*

In this investigation, a docking study of the most potent compounds namely; **5, 13a, 15a, 15b, 17** and **19c** into the ATP binding site of VEGFR-2 kinase was performed using MOE 2014.0901. A high-resolution VEGFR-2 co-crystallized with sunitinib (PDB: 4AGD) [39] was used for docking study. First, sunitinib was docked into the active site of VEGFR-2 enzyme to validate docking procedure. Sunitinib reproduced a binding pose similar to that of the co-crystallized ligand with docking score = −-6.74 kcal/mol. Sunitinib interacts by NH and CO of its indolinone scaffold with the hinge region residues Glu917 and Cys919, respectively, in addition to hydrophobic contacts with Leu840, Ala866, the gatekeeper Val916, Phe918 of the hinge, and Leu1035.

Examining docking results (Figs. 7 and 8), it was found that the analyzed compounds **5, 13a, 15a, 15b, 17, 19c** were well-fitted into the ATP binding site of VEGFR-2 with energy binding scores = −5.41, −6.10, −6.60, −6.70, −4.99, and −5.01 kcal/mol, respectively. Moreover, the docked compounds demonstrated a converged binding pattern similar to that of sunitinib, in which hydrogen bonding interactions with the hinge region key residue Cys919 were observed. It is worth mentioning that the azo linker in

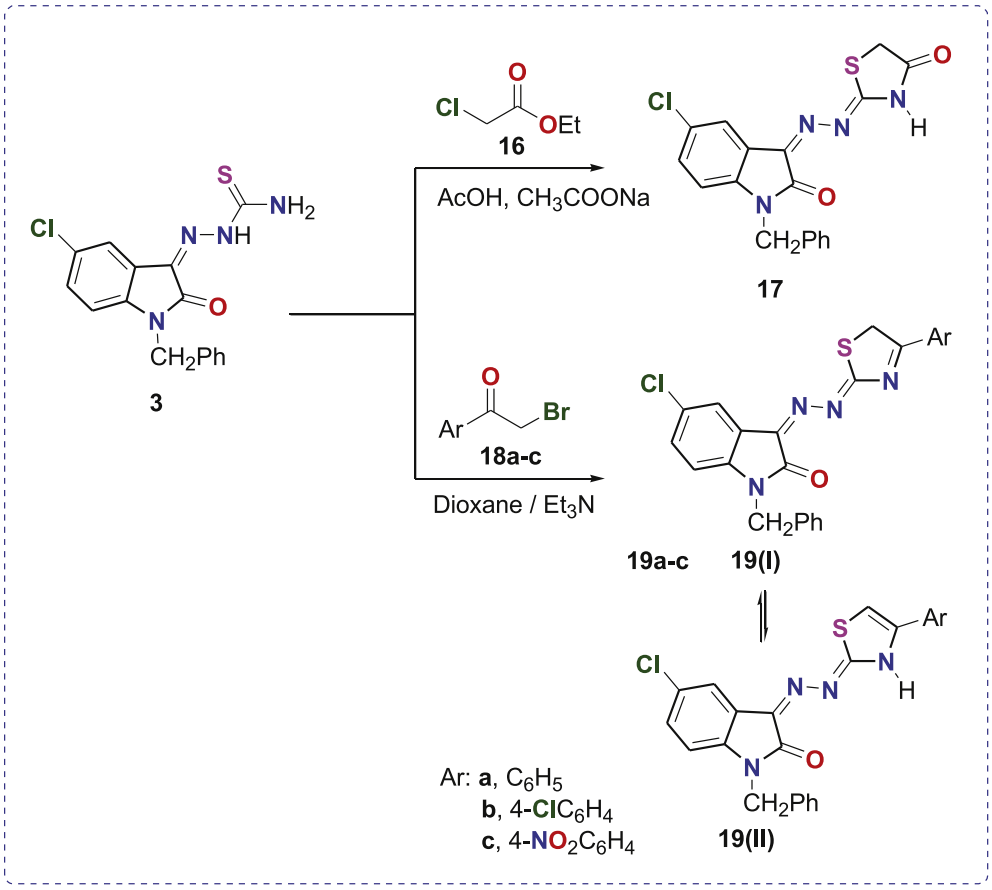

Scheme 5. Synthesis of thiazole derivatives **17** and **19a-c**.

Table 1
VEGFR-2 kinase inhibitory activity of the target compounds.

Comp. No.	IC_{50} (μM)	Comp. No.	IC_{50} (μM)
3	0.174 ± 0.005	**15a**	0.084 ± 0.002
5	0.084 ± 0.002	**15b**	0.092 ± 0.003
10a	0.263 ± 0.007	**17**	0.078 ± 0.002
10b	0.175 ± 0.005	**19a**	0.422 ± 0.001
10c	0.153 ± 0.004	**19b**	0.158 ± 0.004
13a	0.102 ± 0.003	**19c**	0.088 ± 0.002
13b	0.067 ± 0.002	**Sunitinib**	0.075 ± 0.002
13c	0.133 ± 0.004		

Table 2
In vitro anticancer activity of compounds **5, 13b, 15a, 15b, 17** and **19c** against CAKI-1 and A498 renal cancer cell lines.

Comp. No.	Cytotoxicity IC_{50} (μM)	
	CAKI-1	A498
5	0.82 ± 0.03	8.53 ± 0.28
13b	3.9 ± 0.13	2.88 ± 0.09
15a	12.8 ± 0.42	6.27 ± 0.2
15b	3.31 ± 0.11	1.23 ± 0.04
17	35.6 ± 1.16	3.45 ± 0.11
19c	5.78 ± 0.19	24.7 ± 0.8
Sunitinib	4.93 ± 0.16	1.25 ± 0.04

compounds **15a, 15b, 17, 19c** acts as a hydrogen-bond acceptor forming a hydrogen bond with Cys919. Additionally, as planned, benzyl moiety in the docked compounds was fitted into a hydrophobic pocket lined with Leu840, Val848 and Phe1047 residues. This hydrophobic interaction could probably improve the binding affinity of the inhibitors to the VEGFR-2 active site and so could contribute to the high *in vitro* VEGFR-2 inhibitory activity displayed by these compounds.

As seen in Fig. 7A, compound **5** formed two hydrogen bonds with Glu917 and Cys919 through the NH and carbonyl oxygen of its pyrazolone ring, respectively. An intramolecular hydrogen bond was also formed between pyrazole-NH_2 and carbonyl of indolinone core that could further help orient compound **5** within the enzyme active site. Several literatures have described the positive impact of intramolecular hydrogen bonding on ligand-receptor interaction [40].

Additionally, as an H-bond acceptor, carbonyl oxygen of the indolinone core in compound **13b** formed two hydrogen bonds with the hinge Phe918 and Cys919. **13b** was further stabilized within the active site of enzyme *via* an intramolecular hydrogen bond between the azo linker and the tolylhydrazo NH, directing the tolylhdrazo moiety toward the bulk solvent. In addition, benzyl moiety was in a hydrophobic contact with Leu840, Val848 and Phe1047 residues (Fig. 7B). This binding pose could explain the superior anti-VEGFR-2 activity of **13b**.

Considering the binding mode of acetyl thiazole **15a** (Fig. 7C), the azo linker nitrogen accepted one hydrogen bond from Cys919, in addition to the formation of another hydrogen bond between the thiazole ring NH and Glu917. Furthermore, methyl and acetyl groups of thiazole ring were exposed tohydrophobic contacts with gate keeper Val916, Leu840, Val848, Ala866, Val899, and Phe1047.

Focusing on the binding mode of thiazole **15b**; a compound with potent *in vitro* anti-VEGFR-2 activity and superior cytotoxicity, thiazole NH and the azo linker N in compound **15b** formed two hydrogen bonds with the hinge Glu917 and Cys919, respectively.

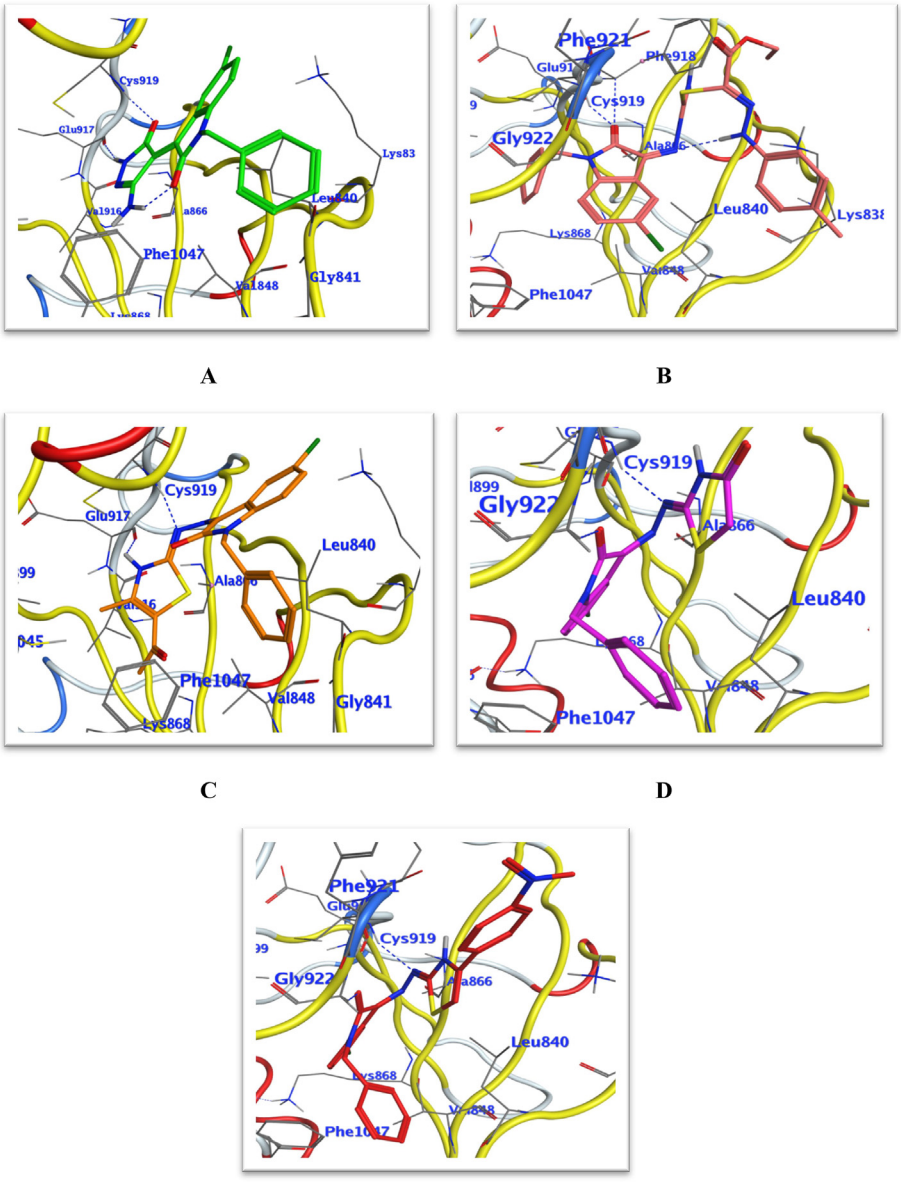

A B C D E

Fig. 7. Compounds **5** (A), **13a** (B), **15a** (C), **17** (D), **19c** (E) docked into the ATP binding site of VEGFR-2.

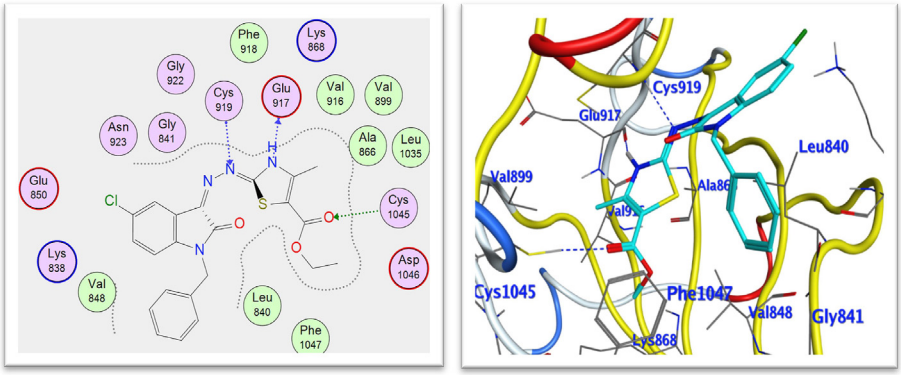

A B

Fig. 8. Compound **15b** docked into the ATP binding site of VEGFR-2; 2D (A), 3D (B).

Moreover, the ester carbonyl oxygen accepted a hydrogen bond from Cys1045 located in the back cleft of the enzyme. Hydrophobic interaction was also observed between the benzyl moiety and Leu840, Val848, and Phe1047 (Fig. 8).

On the other hand, thiazolidinone **17** and thiazole **19c** revealed almost the same binding mode within the active site of VEGFR-2 in which the azo nitrogen and the carbonyl oxygen of indolinone core formed two hydrogen bonds with Cys919 and Gly922, respectively. Besides, benzene ring of indolinone core was exposed to hydrophobic residues; Val848, Ala866, Val918, Phe921, and Leu1035. As well, the benzyl moiety participated in hydrophobic interactions with Leu840, Val848, and Phe1047 (Fig. 7D and E).

Observably, the ability of the docked compounds to bind to the important amino acids within the enzyme active site could rationalize their potent anti-VEGFR-2 activity as indicated by their docking pattern relative to that of sunitinib.

3. Conclusion

Herein, the synthesis of new 2-indolinone thiazole hybrids as sunitinib analogues with potent anti-VEGFR-2 activity has been described. All tested compounds effectively inhibited VEGFR-2 activity with IC_{50} values in the submicromolar level. Compounds **5, 15a, 15b, 17, 19c** displayed excellent VEGFR-2 inhibitory activity, comparable or nearly equipotent to sunitinib. Compound **13b** was the most potent against VEGFR-2 showing IC_{50} value lower than that of sunitinib reference drug. In addition, the most potent compounds were estimated for their anticancer activity against two renal cancer cell lines. The tested compounds exhibited moderate to potent anticancer activity against CAKI-1 and A498 cell lines. Compound **13b** was more potent than sunitinib against CAKI-1 cell line. Moreover, thiazole **15b** was superior/equipotent to sunitinib against CAKI-1/A498 cell lines, respectively. Besides, compound **15b** demonstrated a safety profile much better than that of sunitinib against normal human renal cells. A docking study was also conducted revealing the key interactions essential for VEGFR-2 inhibition.

4. Experimental

4.1. General methods

The melting points of all new 2-indolinone-based thiazole derivatives were recorded using a SMP3 melting point apparatus (the diameter of the glass capillaries is 0.5 mm). The 1430-Perkin-Elmer infrared-spectrophotometer was utilized to record the IR-spectra for all new 2-indolinone-based thiazole derivatives in the range of wavenumber from 4000 cm^{-1} to 200 cm^{-1} as through the formation of sample-KBr discs. The well-known Bruker Avance-300 instrument was utilized to record the H NMR-spectra for all new 2-indolinone-based thiazole derivatives at 300 MHz DMSO-d_6 solutions. Ppm and Hz characterize the chemical shifts (δ) and coupling constants, respectively. To record the molecular weight of all new 2-indolinone-based thiazole derivatives we used a Finnigan-MAT8222 spectrometer at 70 eV in Micro-analytical center at Cairo University. Also, measuring of CHN elemental analyses were investigated on Elementar vario-LIII C—H—N—S analyzer. The starting compounds **2,3** and hydrazonoyl chlorides **7** and **11** were prepared as illustrated in the literature reports [34,41]. The purity of the newly synthesized compounds have been checked by the TLC and further purification of the impure products have been achieved by recrystallization using a proper solvent. The degree of the purity have been tested through the TLC test again and can be estimated from the results of the spectroscopic data. All the synthesized compounds are characterized by high purity before using it in the biological evaluation.

4.2. Synthesis of 3-(3-amino-5-oxo-1H-pyrazol-4(5H)-ylidene)-1-benzyl-5-chloroindolin-2-one (*5*)

Acidified ethanolic solution of 1-benzyl-5-chloroindoline-2,3-dione **2** and freshly prepared cyanoacetic acid hydrazide (0.01 mol of each, 30 mL EtOH and 5 mL AcOH) was subjected to homogenous heating for 5 min. After the solution was left in room temperature to cool, it precipitated orange solid. The formed colored solid was filtered, washed with CH_3OH then crystallized from a mixture of ethanol/dioxane to afford pyrazolyl-5-chloroindolin-2-one derivative **5 as** orange solid, 72% yield, m.p. 178−180 °C; IR (KBr): *v* 3201 (NH, NH_2), 1720 (C═O), 1681 (C═O), 1612 (C═N), 1465, 1357, 1311, 1226, 1157, 1103, 1080, 1033, 1010 cm^{-1}; ^{1}H NMR (DMSO-d_6): δ 4.42 (br, 2H, NH_2), 4.99 (s, 2H, CH_2), 7.05−7.63 (m, 8H, Ar−H), 12.49 (s, 1H, NH), ^{13}C NMR (DMSO-d_6): δ 42.3 (CH_2), 110.5, 116.1, 120.4, 120.7, 123.2, 127.3, 127.4, 127.6, 128.6, 129.4, 131.8, 135.5, 142.8, 160.0 (C═O), 160.2 (C═O). MS *m/z* (%): 354 (M^++2, 14), 353 (M^++1, 9), 352 (M^+, 38). Anal. Calcd for $C_{18}H_{13}ClN_4O_2$ (352.77): C, 61.28; H, 3.71; N, 15.88. Found: C, 61.42; H, 3.69; N, 15.78%.

4.3. Synthesis of compound *10a-c*, *13a-c* and *15a,b*

Reaction of indolinone-thiosemicarbazone derivative **3** (0.34g, 1 mmol) with α-chlorocarbonyl compounds **7a-c, 11a-c or 14a,b** (1 mmol) in 15 mL of dioxane were proceeded under reflux in the presence of 0.35 mL of triethylamine for 5 h. The progress of the reactions were monitored through the TLC test. After the reactions were completed, the solvent was then evaporated under vacuum then washed with CH_3OH. The colored solid produced was filtered and the specific solvent used for each compound for crystallization to give thiazolylhydrazonoindolin-2-one **10a-c, 13a-c** and **15a,b**.

4.3.1. 1-Benzyl-5-chloro-3-((4-methyl-5-(phenyldiazenyl)thiazol-2(3H)-ylidene)hydrazono) -indolin-2-one (*10a*)

Red solid, 86% yield, m.p. 160−162 °C (Dioxane); IR (KBr): *v* 3417 (NH), 1689 (C═O), 1612 (C═N), 1535, 1465, 1373, 1350, 1249, 1157, 1103, 1033 cm^{-1}; ^{1}H NMR (DMSO-d_6): δ 2.67 (s, 3H, CH_3), 4.97 (s, 2H, CH_2), 6.96−7.66 (m, 13H, Ar−H), 11.20 (s, 1H, NH), MS *m/z* (%): 489 (M^++2, 21), 488 (M^++1, 5), 487 (M^+, 69). Anal. Calcd for $C_{25}H_{19}ClN_6OS$ (486.98): C, 61.66; H, 3.93; N, 17.26. Found: C, 61.86; H, 3.72; N, 17.45%.

4.3.2. 1-Benzyl-5-chloro-3-((5-((4-methoxyphenyl)diazenyl)-4-methylthiazol-2(3H)-ylidene)hydrazono)indolin-2-one (*10b*)

Dark red solid, 84% yield, m.p. 198−200 °C (EtOH/dioxane); IR (KBr): *v* 3410 (NH), 1689 (C═O), 1587 (C═N), 1527, 1465, 1435, 1357, 1311, 1249, 1149, 1103, 1033 cm^{-1}; ^{1}H NMR (DMSO-d_6): δ 2.62 (s, 3H, CH_3), 3.82 (s, 3H, OCH_3), 4.99 (s, 2H, CH_2), 6.94−8.33 (m, 12H, Ar−H), 13.19 (s, 1H, NH), MS *m/z* (%): 519 (M^++2, 28), 518 (M^++1, 11), 517 (M^+, 85). Anal. Calcd for $C_{26}H_{21}ClN_6O_2S$ (517.00): C, 60.40; H, 4.09; N, 16.26. Found: C, 60.66; H, 4.18; N, 16.35%

4.3.3. 1-Benzyl-5-chloro-3-((4-methyl-5-(p-tolyldiazenyl)thiazol-2(3H)-ylidene)-hydrazono) -indolin-2-one (*10c*)

Dark red solid, 79% yield, m.p. 214−216 °C (Dioxane); IR (KBr): *v* 3417 (NH), 1681 (C═O), 1612 (C═N), 1535, 1465, 1381, 1357, 1311, 1157, 1103, 1080, 1033, 1010 cm^{-1}; ^{1}H NMR (DMSO-d_6): δ 2.37 (s, 3H, CH_3), 2.65 (s, 3H, CH_3), 4.97 (s, 2H, CH_2), 6.95−7.62 (m, 12H, Ar−H), 13.10 (s, 1H, NH), ^{13}C NMR (DMSO-d_6): δ 14.2 (CH_3), 18.9 (CH_3), 42.1 (CH_2), 114.2, 114.4, 115.5, 115.6, 115.9, 117.1, 118.0, 118.7, 122.8, 124.6, 129.3, 129.6, 129.8, 130.3, 133.3, 142.6, 144.8, 145.9, 163.1 (C═O). MS *m/z* (%): 503 (M^++2, 8), 502 (M^++1, 3), 501 (M^+, 30). Anal. Calcd for

$C_{26}H_{21}ClN_6OS$ (501.00): C, 62.33; H, 4.22; N, 16.77. Found: C, 62.56; H, 4.34; N, 16.92%

4.3.4. N'-(1-benzyl-5-chloro-2-oxoindolin-3-ylidene) carbamohydrazonic-2-ethoxy-N'-(4-nitrophenyl)-2-oxoacetohydrazonic thioanhydride (**13a**)

Orange solid, 76% yield, m.p. 160–162 °C (EtOH); IR (KBr): *ν* 3458 (br. NH_2), 3340 (NH), 3070 (sp^2 CH), 2924 (sp^3 CH), 1720 (C=O), 1681 (CO), 1589 (C=N), 1550, 1473, 1442, 1381, 1357, 1327, 1280, 1257, 1180, 1141, 1103, 1080, 1026 cm^{-1}; ^1H NMR (DMSO-d_6): *δ* 1.33 (t, $J = 7$ Hz, 3H, CH_3), 4.38 (q, $J = 7$ Hz, 2H, CH_2), 3.57 (s, 2H, NH_2), 4.98 (s, 2H, CH_2), 7.01–7.73 (m, 12H, Ar–H), 12.42 (s, 1H, NH). ^{13}C NMR (DMSO-d_6): *δ* 20.7 (CH_3), 42.6 (CH_2), 66.3 (CH2), 109.5, 122.6, 127.2, 127.6, 128.7, 128.9, 136.3, 144.2, 142.7, 142.8, 142.8, 142.9, 143.7, 143.9, 144.1, 144.5, 144.6, 144.7, 158.5 (C=O). MS *m/z* (%): 582 (M^++2, 11), 581 (M^++1, 9), 580 (M^+, 42). Anal. Calcd for $C_{26}H_{22}ClN_7O_5S$ (580.01): C, 53.84; H, 3.82; N, 16.90. Found: C, 53.69; H, 3.71; N, 16.83%.

4.3.5. N'-(1-Benzyl-5-chloro-2-oxoindolin-3-ylidene) carbamohydrazonic-2-ethoxy-2-oxo-N'-(p-tolyl)acetohydrazonic thioanhydride (**13b**)

Orange solid, 85% yield, m.p. 230–232 °C (EtOH/dioxane); IR (KBr): *ν* 3456 (br. NH_2, NH), 1743 (C=O), 1705 (C=O), 1604 (C=N), 1535, 1489, 1465, 1381, 1350, 1288, 1180, 1095, 1056, 1026 cm^{-1}; ^1H NMR (DMSO-d_6): *δ* 1.35 (t, $J = 8$Hz, 3H, CH_3), 2.43 (s, 3H, CH_3), 3.57 (s, 2H, NH_2), 4.42 (q, $J = 8$Hz, 2H, CH_2), 4.94 (s, 2H, CH_2), 6.92–7.92 (m, 13H, Ar–H, NH), MS *m/z* (%): 551 (M^++2, 13), 550 (M^++1, 12), 549 (M^+ 89). Anal. Calcd for $C_{27}H_{25}ClN_6O_3S$ (549.04): C, 59.06; H, 4.59; N, 15.31. Found: C, 59.15; H, 4.42; N, 15.52%

4.3.6. N'-(1-Benzyl-5-chloro-2-oxoindolin-3-ylidene) carbamohydrazonic-N'-(4-bromo-phenyl)-2-ethoxy-2-oxoacetohydrazonic thioanhydride (**13c**)

Orange solid, 87% yield, m.p. 220–222 °C (EtOH); IR (KBr): *ν* 3456 (br. NH_2, NH), 1740 (C=O), 1705 (C=O), 1635 (C=N), 1527, 1489, 1465, 1381, 1350, 1280, 1180, 1095, 1033 cm^{-1}; ^1H NMR (DMSO-d_6): *δ* 1.36 (t, 3H, CH_3), 3.57 (s, 2H, NH_2), 4.40 (q, 2H, CH_2), 4.96 (s, 2H, CH_2), 6.95–7.93 (m, 13H, Ar–H, NH), MS *m/z* (%): 613.91 (M^+). Anal. Calcd for $C_{26}H_{22}BrClN_6O_3S$ (613.91): C, 50.87; H, 3.61; N, 13.69. Found: C, 50.99; H, 3.45; N, 13.82%

4.3.7. 3-((5-Acetyl-4-methylthiazol-2(3H)-ylidene)hydrazono)-1-benzyl-5-chloroindolin-2-one (**15a**)

Orange solid, 91% yield, m.p. 176–178 °C (EtOH); IR (KBr): *ν* 3417 (NH), 1689 (C=O), 1620 (C=O), 1535 (C=N), 1495, 1381, 1350, 1311, 1273, 1203, 1157, 1103, 1080, 1033 cm^{-1}; ^1H NMR (DMSO-d_6): *δ* 2.43 (s, 3H, CH_3), 2.48 (s, 3H, CH_3), 5.0 (s, 2H, CH_2), 6.93–8.32 (m, 8H, Ar–H), 13.20 (s, 1H, NH). ^{13}C NMR (DMSO-d_6): *δ* 14.6 (CH_3), 29.1 (CH_3), 42.4 (CH_2), 110.3, 117.1, 120.1, 120.3, 122.1, 123.1, 126.8, 127.5, 128.5, 130.7, 135.6, 136.5, 141.9, 142.7, 163.9 (C=O), 188.9 (C=O). MS *m/z* (%): 426 (M^++2, 8), 425 (M^++1, 5), 424 (M^+, 26). Anal. Calcd for $C_{21}H_{17}ClN_4O_2S$ (424.90): C, 59.36; H, 4.03; N, 13.19. Found: C, 59.55; H, 4.21; N, 13.32%

4.3.8. Ethyl 2-((1-benzyl-5-chloro-2-oxoindolin-3-ylidene) hydrazono)-4-methyl-2,3-dihydrothiazole-5-carboxylate (**15b**)

Orange solid, 74% yield, m.p. 198–200 °C (EtOH/drops of dioxane); IR (KBr): *ν* 3448 (NH), 1697 (C=O), 1681 (C=O), 1643 (C=N), 1612, 1527, 1465, 1381, 1319, 1265, 1141, 1095, 1033 cm^{-1}; ^1H NMR (DMSO-d_6): *δ* 1.03 (t, $J = 8$Hz, 3H, CH_3), 2.49 (s, 3H, CH_3), 4.24 (q, $J = 8$Hz, 2H, CH_2), 4.99 (s, 2H, CH_2), 6.92–8.30 (m, 8H, Ar–H), 13.16 (s, 1H, NH), MS *m/z* (%): 456 (M^++2, 29), 455 (M^++1, 9), 454 (M^+, 91). Anal. Calcd for $C_{22}H_{19}ClN_4O_3S$ (454.93): C, 58.08; H, 4.21; N, 12.32. Found: C, 58.25; H, 4.33; N, 12.46%

4.4. Synthesis of 2-((1-benzyl-5-chloro-2-oxoindolin-3-ylidene) hydrazono)thiazolidin-4-one (**17**)

Substitution and cyclization reaction of 1 mmol of each of indolinone-thiosemicarbazone derivative **3** and ethylchloroacetate **16** was performed in 20 mL AcOH and 1 mmol of anhydrous sodium acetate after refluxing for 4 h (monitored by TLC). The formed precipitate (isolated after evaporation the acetic acid solvent under vacuum) was washed with cold H_2O, dried and recrystallized from AcOH to give the titled thiazolone derivative **17** as orange solid, with 72% yield, m.p. 240–242 °C (EtOH); IR (KBr): *ν* 3417 (NH), 1720 (C=O), 1620 (C=O), 1535 (C=N), 1465, 1381, 1342, 1242, 1180, 1111, 1033 cm^{-1}; ^1H NMR (DMSO-d_6): *δ* 4.03 (s, 2H, CH_2), 4.95 (s, 2H, CH_2), 6.96–8.29 (m, 8H, Ar–H), 12.45 (s, 1H, NH). ^{13}C NMR (DMSO-d_6): *δ* 33.6 (CH_2), 42.6 (CH_2), 109.6, 116.6, 120.4, 120.8, 122.5, 127.4, 128.3, 129.8, 132.3, 136.1, 143.9, 146.7, 163.6 (C=O), 173.8 (C=O). MS *m/z* (%): 386 (M^++2, 18), 385 (M^++1, 7), 384 (M^+, 61). Anal. Calcd for $C_{18}H_{13}ClN_4O_2S$ (384.84): C, 56.18; H, 3.40; N, 14.56. Found: C, 56.23; H, 3.31; N, 14.42%

4.5. Synthesis of 1-benzyl-5-chloro-3-((substitutedpnenylthiazol-2(3H)-ylidene)hydrazono) -indolin-2-one (**19a-c**)

Reaction of indolinone-thiosemicarbazone derivative **3** (0.34g, 1 mmol) with phenacyl bromide derivatives **18a-c** (1 mmol) in 15 mL of dioxane were proceeded under reflux in the presence of 0.35 mL of trimethylamine for 5 h. The progress of the reactions were monitored through the TLC test. After the reactions were completed, the solvent was then evaporated under vacuum pressure then washed with CH_3OH. The colored solid produced was filtered and recrystallized from the appropriate solvent to give products **19a-c**.

4.5.1. 1-Benzyl-5-chloro-3-((4-phenylthiazol-2(3H)-ylidene) hydrazono)indolin-2-one (**19a**)

Orange solid, 92% yield, m.p. 200–202 °C (EtOH); IR (KBr): *ν* 3471 (NH), 1674 (C=O), 1612 (C=N), 1543, 1465, 1381, 1357, 1273, 1157, 1103, 1033 cm^{-1}; ^1H NMR (DMSO-d_6): *δ* 4.95 (s, 2H, CH_2), 5.04 (s, 2H, CH_2), 7.06–7.93 (m, 13H, Ar–H), MS *m/z* (%): 447 (M^++2, 7), 446 (M^++1, 3), 445 (M^+, 26). Anal. Calcd for $C_{24}H_{17}ClN_4OS$ (444.94): C, 64.79; H, 3.85; N, 12.59. Found: C, 64.57; H, 3.68; N, 12.49%

4.5.2. 1-Benzyl-5-chloro-3-((4-(4-chlorophenyl)thiazol-2(3H)-ylidene)hydrazono)-indolin-2-one (**19b**)

Orange solid, 90% yield, m.p. 208–210 °C (EtOH); *ν* 3464 (NH), 1666 (CO), 1612 (C=N), 1550, 1465, 1380, 1357, 1250, 1165, 1103, 1033, 1010 cm^{-1}; ^1H NMR (DMSO-d_6): *δ* 4.97 (s, 2H, CH_2), 5.04 (s, 2H, CH_2), 7.06–7.95 (m, 12H, Ar–H), MS *m/z* (%): 483 (M^++4, 3), 481 (M^++2, 12), 480 (M^++1, 4), 479 (M^+, 48). Anal. Calcd for $C_{24}H_{16}Cl_2N_4OS$ (479.38): C, 60.13; H, 3.36; N, 11.69 Found: C, 60.24; H, 3.57; N, 11.46%

4.5.3. 1-Benzyl-5-chloro-3-((4-(4-nitrophenyl)thiazol-2(3H)-ylidene)hydrazono)-indolin-2-one (**19c**)

Orange solid, 93% yield, m.p. 260–262 °C (EtOH); *ν* 3417 (NH), 1681 (C=O), 1612 (C=N), 1558, 1504, 1465, 1385, 1342, 1273, 1157, 1103, 1080, 1033, 1002 cm^{-1}; ^1H NMR (DMSO-d_6): *δ* 4.93 (s, 2H, CH_2), 5.02 (s, 2H, CH_2), 7.03–8.26 (m, 12H, Ar–H). ^{13}C NMR (DMSO-d_6): *δ* 42.6 (CH_2), 107.1, 120.0, 121.9, 123.1, 125.6, 125.7, 127.4, 127.6, 128.0, 128.7, 128.9, 130.3, 132.0, 135.8, 139.0, 140.2, 142.5, 142.6, 161.1 (C=O). MS *m/z* (%): 492 (M^++2, 10), 490 (M^+, 63). Anal. Calcd for $C_{24}H_{16}ClN_5O_3S$ (489.93): C, 58.84; H, 3.29; N, 14.29. Found: C, 58.99; H, 3.35; N, 14.46%

4.6. In vitro VEGFR-2 inhibition

The inhibition of VEGFR-2 enzyme was measured using *VEGFR2 Kinase Assay Kit (BIOSCIENCE)*. The *VEGFR2 Kinase Assay Kit* measures VEGFR2 kinase activity for screening applications using Kinase-Glo® MAX as a detection reagent [42]. Percent inhibition was calculated by comparing test compounds to control. The inhibitory concentration 50 was obtained from the concentration-inhibition response curve (n = 3) comparing to sunitinib reference drug.

4.7. In vitro cytotoxicity assay

MTT assay [37] was utilized to evaluate the cytotoxic effect of test compounds using in vitro MTT-based assay kit, Sigma. In brief, A498, CAKI-1 and RPTEC/TERT1 cells; obtained from American Type Culture Collection, were grown in DMEM supplemented with FBS, penicillin and streptomycin and kept under 5% CO_2 at 37 °C. Cells were washed with PBS, collected *via* trypsinization and were plated and incubated under 5% CO_2 at 37 °C overnight. Cells were treated with different concentrations of test compounds and were incubated for 48 h at 37 °C. MTT reagent was added and cells were reincubated for 4 h at 37 °C under dark condition. The absorbance was measured at 590 nm by a plate reader and cell viability was calculated. The inhibitory concentration 50 was obtained from the concentration-inhibition response curve (n = 3), comparing to sunitinib.

Declaration of competing interest

The authors declare that they have no known competing financial interests or personal relationships that could have appeared to influence the work reported in this paper.

Appendix A. Supplementary data

Supplementary data to this article can be found online at https://doi.org/10.1016/j.ejmech.2020.112752.

References

[1] R.L. Siegel, K.D. Miller, A. Jemal, Cancer statistics, 2020, CA Canc. J. Clin. 70 (2020) 7–30, https://doi.org/10.3322/caac.21590.
[2] V.T. DeVita, E. Chu, A history of cancer chemotherapy, Canc. Res. 68 (2008) 8643–8653, https://doi.org/10.1158/0008-5472.CAN-07-6611.
[3] V.V. Padma, An overview of targeted cancer therapy, Biomedicine 5 (2015) 1–6, https://doi.org/10.7603/s40681-015-0019-4.
[4] F. Broekman, E. Giovannetti, G.J. Peters, Tyrosine kinase inhibitors: multi-targeted or single-targeted? World J. Clin. Oncol. 2 (2011) 80–93, https://doi.org/10.5306/wjco.v2.i2.80.
[5] K. Parang, G. Sun, Protein kinase inhibitors drug discovery, in: S.C. Gad (Ed.), Drug Discovery Handbook, John Wiley and Sons, Inc., 2005, pp. 1191–1257, https://doi.org/10.1002/9780470571224.pse027.
[6] M. Pearson, C. García-Echeverría, D. Fabbro, Protein tyrosine kinases as targets for cancer and other indications, in: D. Fabbro, F. Mc Cormick (Eds.), Protein Tyrosine Kinases - from Inhibitors to Useful Drugs, Humana Press Inc., Totowa, New Jersey, 2006, pp. 1–29, https://doi.org/10.1385/1-59259-962-1:001.
[7] P. Carmeliet, VEGF as a key mediator of angiogenesis in cancer, Oncology 69 (2005) 4–10, https://doi.org/10.1159/000088478.
[8] D.J. Hicklin, L.M. Ellis, Role of the vascular endothelial growth factor pathway in tumor growth and angiogenesis, J. Clin. Oncol. 23 (2005) 1011–1027, https://doi.org/10.1200/JCO.2005.06.081.
[9] Z.K. Otrock, J.A. Makarem, A.I. Shamseddine, Vascular endothelial growth factor family of ligands and receptors: review, Blood Cell Mol. Dis. 38 (2007) 258–268, https://doi.org/10.1016/j.bcmd.2006.12.003.
[10] P. Carmeliet, R.K. Jain, Angiogenesis in cancer and other disease, Nature 407 (2000) 249–257, https://doi.org/10.1038/35025220.
[11] L.E. Benjamin, G. Bergers, Tumorigenesis and the angiogenic switch, Nat. Rev. Canc. 3 (2003) 401–410, https://doi.org/10.1038/nrc1093.
[12] R.S. Kerbel, Tumor angiogenesis: past, present and the near future, Carcinogenesis 21 (2000) 505–515, https://doi.org/10.1093/carcin/21.3.505.
[13] K.J. Gotink, H.M.W. Verheul, Anti-angiogenic tyrosine kinase inhibitors:.what is their mechanism of action? Angiogenesis 13 (2010) 1–14, https://doi.org/10.1007/s10456-009-9160-6.
[14] R. Kerbel, J. Folkman, Clinical translation of angiogenesis inhibitors, Nat. Rev. Canc. 2 (2002) 727–739, https://doi.org/10.1038/nrc905.
[15] F. Wang, J. Molina, D. Satele, J. Yin, V.S. Lim, A.A. Adjei, A phase I study of the vascular endothelial growth factor inhibitor vatalanib in combination with pemetrexed disodium in patients with advanced solid tumors, Invest. N. Drugs 37 (2019) 658–665, https://doi.org/10.1007/s10637-018-0690-x.
[16] A. Leoni, A. Locatelli, R. Morigi, M. Rambaldi, 2-Indolinone a Versatile Scaffold for Treatment of Cancer: a Patent Review (2008-2014), Expert Opinion on Therapeutic Patents, 2015, https://doi.org/10.1517/13543776.2016.1118059.
[17] M. Krug, A. Hilgeroth, Recent advances in the development of multi-kinase inhibitors, Mini Rev. Med. Chem. 8 (2008) 1312–1327, https://doi.org/10.2174/138955708786369591.
[18] C.R. Prakash, S. Raja, Indolinones as promising scaffold as kinase inhibitors: a review, Mini Rev. Med. Chem. 12 (2012) 98–119, https://doi.org/10.2174/138955712798995039.
[19] L.Q. Chow, S.G. Eckhardt, Sunitinib: from rational design to clinical efficacy, J. Clin. Oncol. 25 (2007) 884–896, https://doi.org/10.1200/JCO.2006.06.3602.
[20] T.A. Farghaly, G.S. Masaret, Z.A. Muhamm, M.F. Harrasd, Discovery of thiazole-based-chalcones and 4-hetarylthiazoles as potent anticancer agents: synthesis, docking study and anticancer activity, Bioorg. Chem. 98 (2020) 103761, https://doi.org/10.1016/j.bioorg.2020.103761.
[21] I. Althagafi, N.M. El-Metwaly, T.A. Farghaly, Characterization of new Pt(IV)–thiazole complexes: analytical, spectral, molecular modeling and molecular docking studies and applications in two opposing pathways, Appl. Organomet. Chem. (2019) 5099, https://doi.org/10.1002/aoc.5099.
[22] A. Leoni, A. Locatelli, R. Morigi, M. Rambaldi, Novel thiazole derivatives: a patent review (2008-2012. Part 1), Expert Opin. Ther. Pat. 24 (2) (2014) 201–216, https://doi.org/10.1517/13543776.2014.858121.
[23] A. Puszkiel, G. Noé, A. Bellesoeur, et al., Clinical pharmacokinetics and pharmacodynamics of dabrafenib, Clin. Pharmacokinet. 58 (4) (2019) 451–467, https://doi.org/10.1007/s40262-018-0703-0.
[24] G.M. Keating, Dasatinib: a review in chronic myeloid leukaemia and Ph+ acute lymphoblastic leukaemia, Drugs 77 (1) (2017) 85–96, https://doi.org/10.1007/s40265-016-0677-x.
[25] A.M. Gouda, H.A. El-Ghamry, T.M. Bawazeer, T.A. Farghaly, A.N. Abdalla, A. Aslam, Antitumor activity of pyrrolizines and their Cu(II) complexes: design, synthesis and cytotoxic screening with potential apoptosis-inducing activity, Eur. J. Med. Chem. 145 (2018) 350–359, https://doi.org/10.1016/j.ejmech.2018.01.009.
[26] D.H. Dawood, E.M.H. Abbas, T.A. Farghaly, M.M. Ali, M.F. Ibrahim, ZnO nanoparticles catalyst in synthesis of bioactive fused pyrimidines as anti-breast cancer agents targeting VEGFR-2, Med. Chem. 15 (3) (2019) 277–286, https://doi.org/10.2174/1573406414666180912113226.
[27] Z.A. Muhammad, M.A.A. Radwan, T.A. Farghaly, H.M. Gaber, M.M. Elaasser, Synthesis and antitumor activity of novel [1,2,4,5]-tetrazepino[6,7-b]indole derivatives: marine natural product Hyrtioreticuline C and D analogues, Mini Rev. Med. Chem. 19 (1) (2019) 79–86, https://doi.org/10.2174/1389557518666180724094244.
[28] A.M.R. Alsaedi, T.A. Farghaly, M.R. Shaaban, Synthesis and antimicrobial evaluation of novel pyrazolopyrimidines incorporated with mono- and diphenylsulfonyl groups, Molecules 24 (2019) 4009, https://doi.org/10.3390/molecules24214009.
[29] S.F. Mohamed, E.M.H. Abbas, H.S. Khalaf, T.A. Farghaly, D.N. Abd El-Shafy, Triazolopyrimidines and thiazolopyrimidines: synthesis, anti-HSV-1, cytotoxicity and mechanism of action, Mini Rev. Med. Chem. 18 (2018) 794–802, https://doi.org/10.2174/1389557518666171207161542.
[30] T.A. Farghaly, M.A. Abdallah, G.S. Masaret, Z.A. Muhammad, New and efficient approach for synthesis of novel bioactive [1,3,4]thiadiazoles incorporated with 1,3-thiazole moiety, Eur. J. Med. Chem. (2015) 320–333, https://doi.org/10.1016/j.ejmech.2015.05.009.
[31] R. Roskoski Jr., Classification of small molecule protein kinase inhibitors based upon the structures of their drug-enzyme complexes, Pharmacol. Res. 103 (2016) 26–48, https://doi.org/10.1016/j.phrs.2015.10.021.
[32] W.M. Eldehna, S.M. Abou-Seri, A.M. El Kerdawy, R.R. Ayyad, A.M. Hamdy, H.A. Ghabbour, M.M. Ali, D.A. Abou El Ella, Increasing the binding affinity of VEGFR-2 inhibitors by extending their hydrophobic interaction with the active site: design, synthesis and biological evaluation of 1-substituted-4-(4-methoxybenzyl)phthalazine derivatives, Eur. J. Med. Chem. 113 (2016) 50–62, https://doi.org/10.1016/j.ejmech.2016.02.029.
[33] W.M. Eldehna, A.M. El Kerdawy, G.H. Al-Ansary, S.T. Al-Rashood, M.M. Ali, A.E. Mahmoud, Type IIA - type IIB protein tyrosine kinase inhibitors hybridization as an efficient approach for potent multikinase inhibitor development: design, synthesis, anti-proliferative activity, multikinase inhibitory activity and molecular modeling of novel indolinone-based ureides and amides, Eur. J. Med. Chem. 163 (2019) 37–53, https://doi.org/10.1016/j.ejmech.2018.11.061.
[34] S.S. Kari, V.S. Bahaduria, V. Rana, S. Kumar, P.G. Subbaro, U. Das, J. Balzarini, E. De Clercq, J.R. Dimmock, 1-Arylmethyl-2,3-dioxo-2,3-dihydroindole thiosemicarbazones as leads for developing cytotoxins and anticonvulsants, J. Enzym. Inhib. Med. Chem. 24 (2) (2009) 537–544.
[35] R. Roskoski Jr., Properties of FDA-approved small molecule protein kinase inhibitors: a 2020 update, Pharmacol. Res. 152 (2020) 104609, https://doi.org/10.1016/j.phrs.2019.104609.
[36] R. Roskoski Jr., Vascular endothelial growth factor (VEGF) signaling in tumor progression, Crit. Rev. Oncol. Hematol. 62 (2007) 179–213, https://doi.org/

10.1016/j.critrevonc.2007.01.006.
[37] T. Mosmann, Rapid colorimetric assay for cellular growth and survival: application to proliferation and cytotoxicity assays, J. Immunol. Methods 65 (1983) 55–63, https://doi.org/10.1016/0022-1759(83)90303-4.
[38] K.K. Brodaczewska, C. Szczylik, M. Fiedorowicz, C. Porta, A.M. Czarnecka, Choosing the right cell line for renal cell cancer research, Mol. Canc. 15 (1) (2016) 83, https://doi.org/10.1186/s12943-016-0565-8.
[39] M. Mctigue, B.W. Murray, J.H. Chen, Y. Deng, J. Solowiej, R.S. Kania, Molecular conformations, interactions, and properties associated with drug efficiency and clinical performance among Vegfr tk inhibitors, Proc. Natl. Acad. Sci. U. S. A. 109 (2012) 18281, https://doi.org/10.1073/pnas.1207759109.
[40] M.J.R. Yunta, It is important to compute intramolecular hydrogen bonding in drug design? Am. J. Model. Optim. 5 (1) (2017) 24–57, https://doi.org/10.12691/ajmo-5-1-3.
[41] A.S. Shawali, H.A. Albar, Kinetics and mechanism of dehydrochlorination of N-aryl-C-ethoxycarbonylformohydrazidoylchlorides, Can. J. Chem. 64 (1986) 871–875, https://doi.org/10.1139/v86-144.
[42] K. Sharma, P.S. Suresh, R. Mullangi, N.R. Srinivas, Quantitation of VEGFR2 (vascular endothelial growth factor receptor) inhibitors-review of assay methodologies and perspectives, Biomed. Chromatogr. 29 (6) (2015) 803–834, https://doi.org/10.1002/bmc.3370.